Science of the Total Environment 650 (2019) 155–162

Contents lists available at ScienceDirect

Science of the Total Environment

journal homepage: www.elsevier.com/locate/scitotenv

Robust spatial analysis of sequestered metals in a Southern California Bioswale

Natalya Evans[a,*], Hal Van Ryswyk[a], Marc Los Huertos[b], Tanja Srebotnjak[a]

[a] Harvey Mudd College, 301 Platt Blvd, Claremont, CA 91711, United States of America
[b] Pomona College, Sumner Hall, 333 N College Way, Claremont, CA 91711, United States of America

HIGHLIGHTS

- Zn, Pb, Co, Cu, and Mn sequestered with statistical significance in the bioswale.
- Sequestered metals have elevated concentration in the carbonate soil fraction.
- A metal's introduction via runoff or aerosol dictates its spatial distribution in the bioswale

GRAPHICAL ABSTRACT

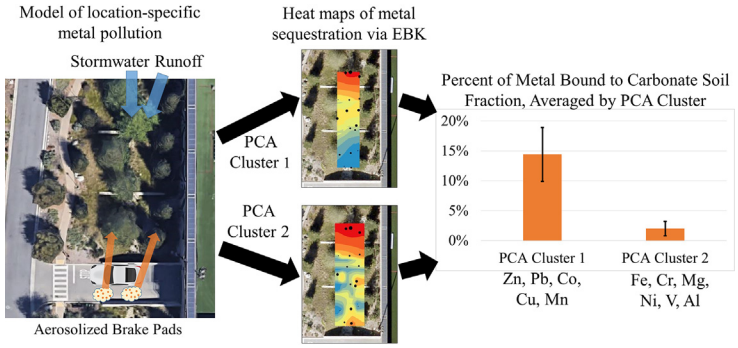

ARTICLE INFO

Article history:
Received 2 May 2018
Received in revised form 22 August 2018
Accepted 31 August 2018
Available online 1 September 2018

Editor: F.M. Tack

Keywords:
Heavy metals
Empirical Bayesian Kriging
Bioswale
Sequential extraction
Principal component analysis

ABSTRACT

Bioswales are a type of permeable green infrastructure designed to slow stormwater and clean runoff by sequestering pollutants such as heavy metals. Measurements of dissolved pollutants before and after the bioswale often justify their ability to clean this runoff, but research addressing the physical and chemical sequestration of these pollutants is scarce. Soil samples were taken from an arid bioswale and analyzed for concentrations of aluminum, cobalt, chromium, copper, iron, magnesium, manganese, nickel, lead, vanadium and zinc. Heat maps of the concentration of these metals in soil were generated via Empirical Bayesian Kriging (EBK) and demonstrate that location-specific sequestration differs between metals within the same swale. Sequential extraction with a modified Tessier et al. (1979) protocol coupled with profiles of metal concentration versus distance along the main flow axis in the bioswale illustrate that the carbonate soil fraction contains elevated concentrations of zinc, lead, cobalt, and manganese, metals sequestered by the bioswale with statistical significance.

1. Background

Many studies have quantified the efficiency of various types of biofilters at remediating road runoff by comparing the concentration of metals in the inflow versus the outflow (Anderson et al., 2016, Leroy et al., 2016, Blecken et al., 2009, Chapman and Horner, 2010, Davis, 2007, Hatt et al., 2009, Hunt et al., 2008). While these papers demonstrate that bioswales sequester pollutants such as hydrocarbons, zinc, cadmium, lead, as well as mitigate peak runoff, fewer papers have examined the location-specific sequestration of metals in these biofilters. Papers that discuss location tend to characterize a large area of land (Annu et al., 2016) rather than study the behavior of metals

* Corresponding author at: Department of Chemistry, Harvey Mudd College, 301 Platt Blvd., Claremont, CA 91711, United States of America.
E-mail address: n.evans@usc.edu (N. Evans).

https://doi.org/10.1016/j.scitotenv.2018.08.441
0048-9697/

Abbreviations

PCA	Principal Component Analysis
EBK	Empirical Bayesian Kriging
ICP-OES	Inductively-Coupled Plasma Optical Emission Spectroscopy

themselves. Identifying spatial patterns and chemical trends for metal sequestration in this bioswale allows patterns to be drawn between metals that are sequestered more efficiently in the bioswale and the components of the bioswale soil that drive this sequestration.

This study aims to identify the spatial sequestration patterns of and soil fractions responsible for metal sequestration within this bioswale. Previous work by Lewis et al. (2016) demonstrated that most metals in runoff decrease in concentration along the bioswale, but they did not analyze the sequestration of these metals. Analysis by soil fraction is often used to describe the remediation of soil (Almeida et al., 2004; Georgiev et al., 2016), because these soil fractions have varying strength of metal retention due to different chemical processes of adsorption. The exchangeable fraction is described as metals dissolved through ionic activity, and it is the weakest-bound fraction. The carbonate fraction is sensitive to acidic pH levels, and metals within this fraction are usually less available than the exchangeable fraction. The iron/manganese oxide fraction is bound to mineral surfaces. This soil fraction exists in between and around granules of soil, is the least available sample extracted, and is sensitive to anoxic conditions. The organic fraction is the most tightly bound fraction, and the availability of metals bound to it decreases compared to the iron/manganese oxide fraction (Tessier et al., 1979). This analysis of the distribution of metals between soil fractions, while used frequently with remediation, is rarely paired with the transport of metals through a biofilter. Coupling these measurements allows for the identification of soil fractions correlated with elevated metal sequestration.

Available studies on metal remediation in soil typically select a few heavy metals of environmental significance, such as zinc, lead, and cadmium as presented in Li et al., 2016 and Leroy et al., 2016. Subsets of metals such as these are often presented as representative of heavy metals or anthropogenic metals (Anderson et al., 2016, Delgard et al., 2012, Georgiev et al., 2016, Blecken et al., 2009, Davis, 2007, Hatt et al., 2009, Hunt et al., 2008). Despite this trend, atomic emission spectroscopy allows for the simultaneous quantification of an expanded group of metals, which can provide insight into the unique pathways by which various metals may be introduced, distributed between soil fractions, and sequestered with different efficiencies. Grant et al. (2003) has identified the methods of introduction of various metals from automobiles, such as oil containing zinc and therefore zinc being displaced in road runoff, as compared to chromium being emitted through brake aerosols. The present study analyzes the spatial sequestration of metals in a bioswale via heats maps based on Empirical Bayesian Kriging and demonstrates how the methods of metal introduction and the distribution of metals within soil fractions influences the group of metals the bioswale sequesters.

2. Methods

2.1. Site description

The Pomona College bioswale in Claremont, CA was completed in 2012 in conjunction with the construction of a new parking garage on Columbia Avenue. It receives runoff from approximately 30 km^2, conservatively, of a residential, suburban college campus, including 26 km of streets (Lewis et al., 2016). This study focuses on the three catchment basins on the west side of the bioswale (Fig. 1), because previous observations found that they receive higher water flow than the east side. The bioswale consists of approximately 15 cm of topsoil above clay. Runoff enters the bioswale from the north through two inflow pipes, then flows south longitudinally through the bioswale. The center inflow pipe carries primarily road runoff, whereas the more eastern inflow pipe carries runoff from the adjacent parking garage and AstroTurf roof, where the AstroTurf is made from recycled tires. The stormwater then flows through a series of three catchment basins separated by two river rock berms that were implemented to slow water flow as seen in Fig. 1a. Each catchment basin contains three distinct vegetative and design areas: the west side has white alder (*Alnus rhombifolia*), the middle section is rocky and is the lowest area, designed for water to flow, and the east side is filled with native *Carex* sedge, as seen in Fig. 1b. Vegetation includes other native plants such as Elk Blue (*Juncus patens*) and *Epilobium ciliatum* subsp. *Ciliatum* as well as non-native species of date palm (*Phoenix dactylifera*).

2.2. Sampling design and chemical analysis

Sampling locations were measured with a Trimble GeoXT GPS unit, providing a median precision of 50 cm. To profile metal concentrations in the bioswale, the west, middle, and east flow paths were sampled in an approximately regular grid with interval length of three meters, starting with three samples in the first catchment basin, nine in the second catchment basin, and six in the third catchment basin. The majority of samples were removed at the surface of the soil (0–5 cm deep, below leaf litter) as well as several depth samples at 5–15 cm and 15–25 cm below surface. Samples were acquired by collecting approximately 20 g of soil from several places within a 10 cm radius around a central point and sieving three times with a 20 mesh 0.833 mm size sieve. Pseudo-total metal concentrations were obtained using microwave-assisted digestion in nitric acid as specified by EPA Method 3051 using a CEM MARS Xpress at Harvey Mudd College, California and filtered with a 13 mm diameter, 2-μm glass fiber filter (Millipore Sigma AP2501300) using a Hirsch funnel. While this method does not measure the residual metal fraction, runoff metals are unlikely to become mineralized into the residual fraction within a younger bioswale. All samples received 10 mL of nitric acid. After digestion, samples were filtered, diluted to 25 mL with deionized water, and stored in poly(propylene) test tubes for processing via PerkinElmer Optima 8300 ICP-OES at Keck Science Department, California. The plasma operated at 1500 W RF power with argon gas flows of 10 L/min, 0.4 L/min, and 0.6 L/min in plasma, auxiliary, and nebulizer, respectively. A five-point standard consisting of 0.01 ppm, 0.1 ppm, 1.0 ppm, 10 ppm, and 100 ppm for aluminum, cadmium, chromium, cobalt, copper, iron, lead, magnesium, manganese, mercury, nickel, silver, thallium, vanadium, and zinc with an additional 500 ppm aluminum and iron standard were used. These standards were made from a VWR Transition Metal Group standard modified with a known concentration of aluminum and iron, and spectra were acquired axially for the lowest detection limits and fit linearly through zero.

In addition, a sequential extraction procedure modified from Tessier et al. (1979) was used to characterize the distribution of metals bound to the exchangeable, carbonate, iron-manganese oxide, and organic fractions. Sequential extraction begin with 1 g of soil dried in an oven at 50 °C or above overnight, and the exchangeable fraction was extracted by adding 8 mL of 1 M sodium acetate with pH adjusted to 8.2 for 1 h in an incubator at 250 rpm and 25 °C. Samples were centrifuged at 12,100g for 30 min after digestion, remaining soil filtered off using a 30 mm diameter, 80 μm quantitative analysis cotton linter filter (Millipore Sigma Z752630) using a Büchner funnel, and diluted to 50 mL with deionized water. After removing soil, it was dried overnight and massed for the next round of extraction. Almeida et al. (2004) indicated that drying the soil did not affect sequential extraction results, and hence the soils were dried before the next extraction. The carbonate fraction was extracted by adding 8 mL of 1 M sodium acetate with pH adjusted to 5.0 with acetic acid for 5 h in a shaking incubator at 250 rpm and 25 °C. The sample was centrifuged, filtered, and soil was

Fig. 1. (a) Diagram of Pomona College bioswale (Lewis et al., 2016), (b) Aerial photo with direction of flow path indicated along rocky section, and (c) Map marking bioswale location within the Claremont Colleges and surrounding area.

dried as described above. The iron-manganese oxide fraction was extracted by adding 20 mL of 0.04 M hydroxylamine hydrochloride in 25% (v/w) acetic acid for 6 h in a shaking incubator at 50 rpm and 80 °C. The Tessier et al. (1979) procedure calls for 96 °C, but available equipment was incapable of reaching that temperature. After centrifugation, filtration, and drying, the organic fraction was extracted using the EPA 3051 technique instead of the step Tessier et al. (1979) describes due to similarity in procedures and convenience.

2.3. Data analysis

Prior to data analysis, the cadmium, mercury, and thallium concentrations were excluded because they were below the 10 ppm limit of quantification. The measurements for silver were removed due to contamination, and several outliers with negative values were edited to zero. Linear regression models and the Principal Component Analysis (PCA) were implemented in the R statistical computing language (R Development Core Team, 2008) version 3.0.2 and using Rstudio version 0.99.982. Metal concentrations were binned using Jenks Natural Breaks and Empirical Bayesian Kriging (EBK) was done in ArcMap Version 10.4 to obtain heat maps of the distribution of metal concentrations across the bioswale. The assumptions for using linear regressions and Bayesian Kriging analysis were verified with sample probability distribution plots, Q-Q plots, and Thiessen polygons. The EBK semi-variograms were fit with a power model.

3. Results and discussion

To view the decrease of these metals along the bioswale, Empirical Bayesian Kriging was used to estimate the concentration field between sampling locations for each metal (Fig. 2). Significance of surface metal

sequestration was then determined with p-values from a linear regression model of metal concentration versus distance along the main flow axis of the bioswale (Table S1), which is north to south and measured with latitude.

Zinc, lead, cobalt, copper, and manganese show clear decrease in metal concentration along the flow path of the bioswale upon entering the bioswale as runoff through the upper two inflow pipes. A previous study identified that dissolved transition metal concentrations were

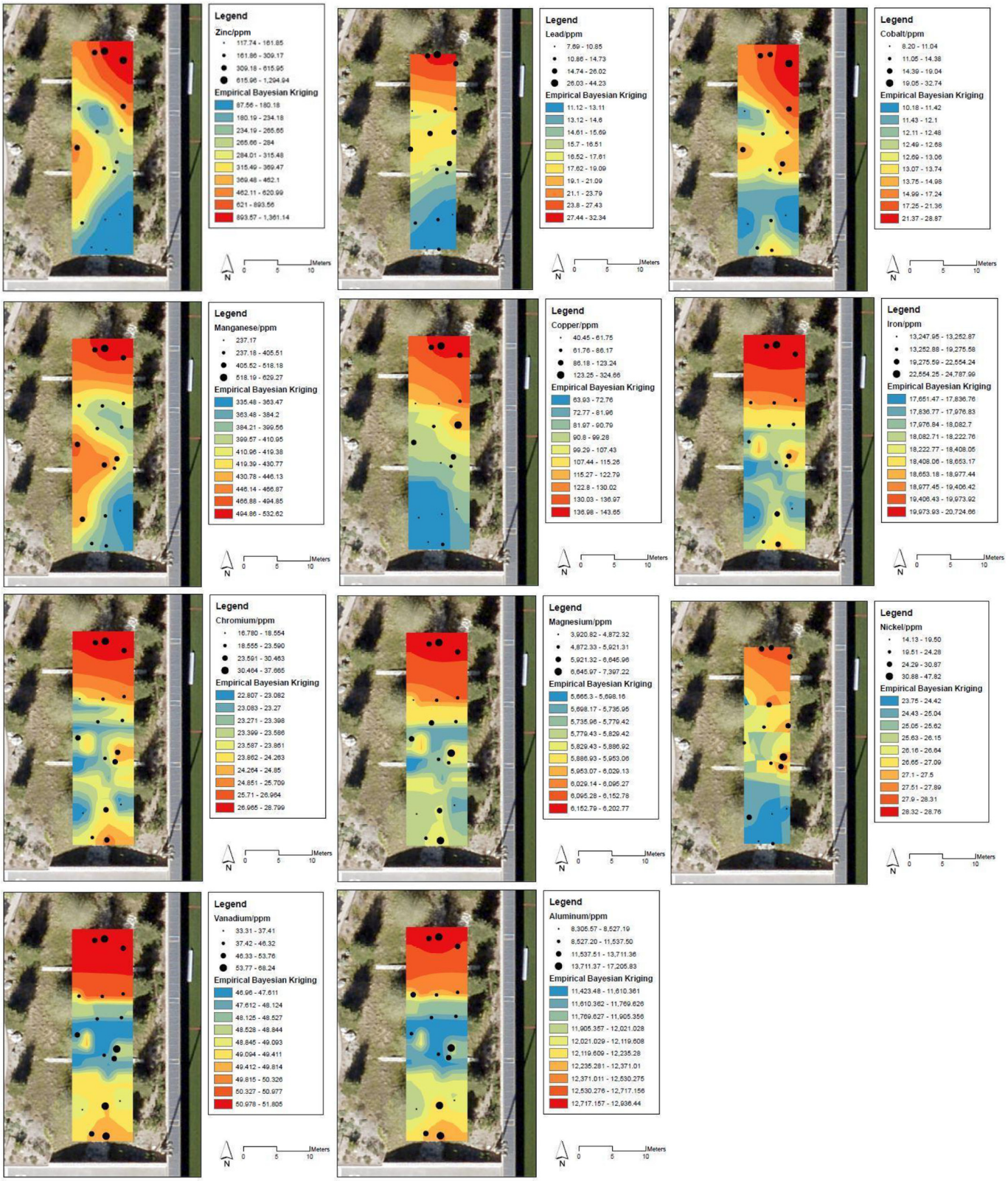

Fig. 2. Bayesian Empirical Kriging results for each metal superimposed on bioswale aerial photo, in order of decreasing statistical significance. The results for zinc, lead and cobalt showed the greatest decline in concentrations along latitude. The points indicate sampling locations and their areas are proportional to the measured concentration, binned via Jenks Natural Breaks.

highest in effluent water from these inflows compared to inter-basin and outflow samples (Lewis et al., 2016). Lead and zinc are known contaminants from tire wear and hence associated with road runoff. Zinc is found in motor oil and grease, which is more prolific than the particulates released by tire wear (Grant et al., 2003) and could justify the significant entry of zinc from the west compared to the slighter increase of lead concentrations. Since the eastern inflow pipe releases runoff from inside the parking garage, it is likely that accumulated leaks of motor oil in the parking garage lead to the higher sequestration of zinc in the upper east corner of the bioswale.

In road runoff, cobalt is only found on waste from tire manufacturing, not the brakes, grease, or oil (Grant et al., 2003). Since cobalt enters the bioswale primarily through runoff from the parking garage, it likely originates from the recycled tires used to make the AstroTurf field on top of the parking garage. There also appears to be some contribution from other sources, likely non-road runoff, that flow out of the western boundary road and into the bioswale. Copper is released in bearing and brake pad wear (Grant et al., 2003), and its distribution is noticeably different from zinc, cobalt, and manganese because it does not enter the bioswale from the western road. Grant et al., 2003 does not specify a source for manganese in road runoff, but its sequestration appears well-correlated with zinc. The Jenks binning method resulted in one class in manganese to have only one observation rather than a range. This is likely due to the significant northern and western inflows reducing the number of manganese minima to one, unlike other metals with several.

Aluminum, vanadium, magnesium, chromium, and iron appear in elevated concentrations in the northern and southern sections of the bioswale. Although the main flow axis of the bioswale is north-south with entry in the north, the EBK-generated concentration surfaces indicate that some metals enter the bioswale through smaller inflows from the west and east sides as well.

The Principal Component Analysis (PCA) clustered this set of metals separately into two groups along PCA dimension 2: zinc, cobalt, copper, lead, and manganese versus chromium, iron, aluminum, magnesium, and vanadium (Fig. 3, lower left-hand corner). This indicates a different distribution in the surface soil of the bioswale between these metals. The metals seen in cluster 1, the first quadrant of the PCA component map, have the most significant p-values in simple linear regression fits. Zinc, lead, and cobalt are highly statistically significant ($p < 0.05$), while copper and manganese are marginally significant ($p < 0.1$).

The only metal not clustered into these two groups is nickel. Nickel is released through diesel fuel and gasoline (Grant et al., 2003), and the highly-aerosolized nature of these compounds likely contributes to this noisy distribution in its EBK heat map and its neutral loading on PCA dimension 2. Nickel concentration differs between the top 5 cm of soil and the subsequent 5 cm of soil with statistical significance ($p < 0.02$), while all other metals lack statistically significant difference between these soil layers.

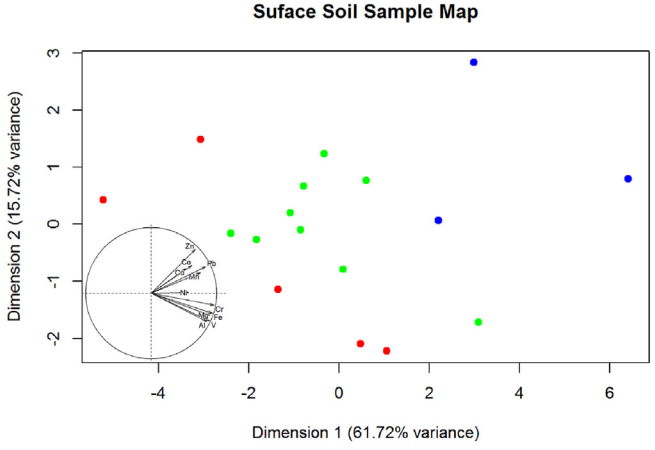

Fig. 3. Results of PCA for selected metal concentrations. The lower left corner depicts the loading of the metals according to the first and second dimensions as projected onto orthogonal x- and y-axes. Legend: blue: first catchment basin; green: second catchment basin; red: third catchment basin.

Metals in cluster 2, as seen in the fourth quadrant of the PCA component figure, tend to have minima in the middle of the bioswale rather than the bottom, as compared to metals in cluster 1, which monotonically decrease. This trend in metals belonging to cluster 2 may be caused by the method of introduction of these metals into the bioswale. Most of these metals are present on the brake pads, bearings, and/or tires of cars and could be primarily released through brake lining wear (Grant et al., 2003). This process would aerosolize metals such as chromium, copper and nickel from brake pads, bearings, and tires. The bottom of the third catchment basin borders the only driveway into the parking garage, and aerosolized metals could be released upon drivers applying brakes as they enter the parking garage. Previous, preliminary measurements by Lewis et al. (2016) on dissolved metal concentrations during two storm events indicate that metals in cluster 1 strictly decrease between the inflow, check dams, and outflow, whereas iron, magnesium and nickel reveal some increase in concentration. This increase in dissolved metal concentration is likely due to the non-monotonic soil sequestration of metals seen in cluster 2. Nickel, which does not contribute to either cluster, is the only metal contained solely in fuel (Grant et al., 2003). Therefore, it could be introduced through long distance aerosols in exhaust compared with brake lining aerosols, which likely cover a shorter distance due to the height of emission.

Linear regression models were fit for each metal's concentrations as a function of the samples' latitude within the bioswale, as a proxy for distance down the bioswale, to confirm the clustering identified by the PCA results. Since metals differ in their abundance in soil, e.g., iron is more prevalent than chromium, p-values were used as indicators of how significantly the metal's concentration decreases across the bioswale's axis of water flow. Using this linear regression analysis, zinc, lead, and copper were found to be statistically significant ($p < 0.05$) while copper and manganese were found to be approaching statistical significance ($p < 0.10$). The statistical significance of metal concentration decreasing in surface soil matches the clustering generated in PCA, and linear regression results can be seen in the supplemental information.

In addition to using the EPA 3051 protocol for pseudo-total metal extraction, a sequential extraction technique was used to analyze the distribution of metals between different soil fractions, as the distribution in soil fractions hints at the chemistry of bioremediation, as demonstrated in Georgiev et al. (2016). Sequential extraction was initially used to investigate differences between bulk and rhizosphere soil as well as the role of depth in depth samples. The differences between bulk and rhizosphere as well as depth were minimal with respect to distribution of metals in soil fractions. Nevertheless, the analysis demonstrated that metals in the soil of the bioswale are primarily bound to the organic fraction, albeit to varying extent as seen in Fig. 4.

Fig. 4 displays the average distribution of metals within soil fractions of the bioswale. Among the metals that showed a statistically significant decrease in concentration along the main flow axis of the bioswale – zinc, lead, cobalt, manganese and copper – the first four metals are found at a comparatively smaller percentage in the organic fraction than the metals with non-uniformly declining concentrations along the flow axis. Copper, however, breaks this trend.

The organic fraction is the most tightly bound (Tessier et al., 1979), i.e., metals that partition less into that fraction may be more mobile. When comparing the percentage of metals in the organic fraction, metals that have no statistical variation across the bioswale such as aluminum, vanadium, and magnesium are more present in the organic soil fraction. These metals display lower concentrations in the carbonate soil fraction as compared to metals that are sequestered effectively into the soil of the bioswale. While there is some difference in affinity between

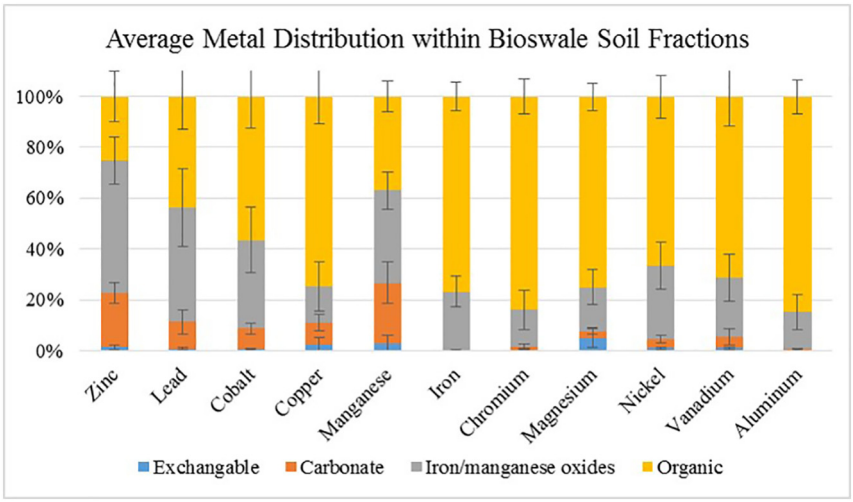

Fig. 4. Average of sequential extractions of six soil samples. Amount of metal in each fraction has been normalized due to large differences between concentrations of metals, and error bars are the standard deviation in percentage. Metals are displayed in order of increasing p-value, or decreasing statistical significance of sequestration along the flow path of the bioswale.

these groups of metals in the iron/manganese oxide soil fraction, which is notable for strong sequestration of trace metals (Gadde and Laitinen, 1974) and (Brown et al., 1999), this soil fraction lacks the significant difference between the two clusters of metals seen in Fig. 5.

When the percentage of each metal in the carbonate fraction is compared across catchment basins as displayed in Fig. 6, there is a noticeable decrease in the percentage of each PCA cluster 1 metal across the catchment basins, with the exception of copper. Metals to the left of iron are sequestered with statistical significance and compose the first PCA cluster. In addition, there is relatively little or even the opposite trend for metals that did not sequester with statistical significance in the bioswale.

Fig. 6 suggests that elevated concentrations of cluster 1 metals besides copper are retained by carbonates in the soil, such that this soil fraction could be responsible for the statistical significance of the sequestration of these metals. While the percent of zinc bound to the carbonate fraction appears to increase from the first catchment basin to the second, the standard deviation of these measurements render this nuance unlikely. Cobalt's large standard deviation in the first catchment basin is caused by averaging its eastern entry point and the lower concentration points west of this point in the first catchment basin, and this large standard deviation inflates the standard deviation in the third catchment basin. Copper's extremely high affinity for organic complexes (Kogut and Voelker, 2003) likely causes it to be an outlier from the cluster 1 trend, since it preferentially binds with organic material before carbonates such that the high carbonate percent only appears at the low copper concentrations in the third catchment basin.

The second cluster of metals with lower concentrations in the carbonate soil fraction, as seen in Fig. 5, appears to follow the opposite trend of carbonate percentage versus catchment basin. Should these metals partition away from the carbonate soil fraction, then the percentage of these metals in the carbonate fraction will likely increase as their concentration decreases because the amount of metal bound to preferred fractions decreases with total metal concentration. The low concentrations of these metals in the carbonate soil fraction interferes with the clarity of this trend, though it can be seen with iron, chromium, and magnesium. In addition, the cause for nickel's decrease in the second catchment basin is unknown, the standard deviation of vanadium's second catchment basin percentage challenge its analysis, and aluminum's percentage is too low to analyze with confidence.

The correlation of metals sequestered efficiently by the bioswale and elevated levels of these metals in the carbonate soil fraction suggest that

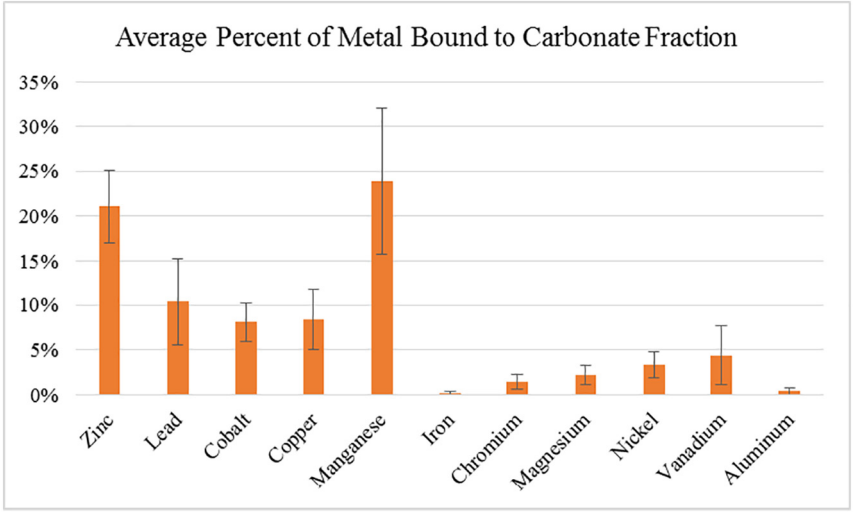

Fig. 5. Average of percent of each metal found in the carbonate fraction during sequential extraction. Metals are displayed in order of increasing p-value, or decreasing statistical significance of sequestration along the flow path of the bioswale. Metals to the left, non-inclusive, of iron are sequestered with statistical significance and compose the first PCA cluster in quadrant 1. The amount of metal has been normalized due to large differences in metals abundance, and error bars are the standard deviation in percentage.

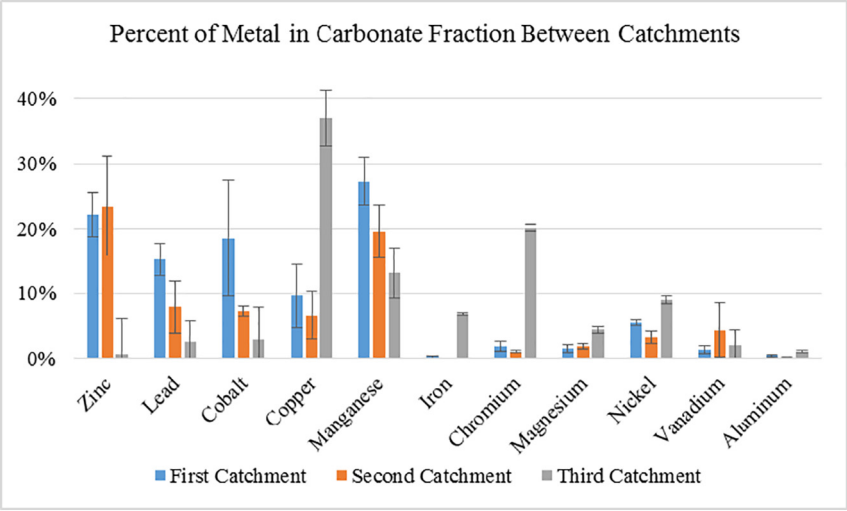

Fig. 6. The components of Fig. 5, Average Percent of Metal in Carbonate Soil Fraction, can be deconvoluted into catchment basins to examine how the percent of metal in the carbonate fraction varies based on location. Each bar represents the percent of that metal found in the carbonate fraction during sequential extraction of soil from that catchment basin. Metals are displayed in order of increasing p-value, or decreasing statistical significance of sequestration along the flow path of the bioswale. The amount of metal has been normalized due to large differences in metals abundance, and error bars are the standard deviation in percentage. Due to a limited number of samples in the third catchment basin, error bars for the third catchment basin are the averages of the standard deviations of that metal in the first and second catchment basin.

the carbonate soil fraction likely contributes to this statistically significant sequestration. Nevertheless, the role of aqueous runoff versus aerosol introduction of these metals also influences their spatial sequestration pattern, such that both introduction via road runoff and increased affinity to the carbonate soil fraction likely contribute to the sequestration efficiency of zinc, lead, cobalt, copper, and manganese.

The study has a number of limitations. The empirical results are limited to the Pomona College bioswale, which was finished in 2014 and is therefore not yet mature. Its exposure to road runoff and other sources of point and non-point pollution are also limited. For these reasons, the measured concentrations of typical storm runoff pollutants are likely below those seen near older, busier roadways. The study selected a wide range of metals but had to exclude cadmium, mercury, and thallium due to measurements below quantification level and silver due to sample contamination. The sequential extraction performed uses artificial delineations of soil fractions and low repeatability protocols, rendering the technique more useful for trend analysis than absolute measurements (Zimmerman and Weindorf, 2010). In addition, the limited number and possible depth of depth samples also render an analysis of infiltration of metals into groundwater difficult to model, though deviation of depth samples from surface samples is apparent with PCA.

4. Conclusions

This study aimed to gain better understanding of the ability of bioswales to sequester metals, using a combination of Empirical Bayesian Kriging, Principal Component Analysis, regression modeling, and sequential extraction analysis. It examined how and which metals are sequestered as a function of latitude, as a proxy for distance along the flow path of the bioswale; depth; and soil fraction. While there are many studies on the percentage of metals that suggest bioswales and other biofilters manage to reduce between inflow and outflow, the location-specific sequestration of metals is not studied as widely. The EBK results indicate that almost all metals are sequestered within the first catchment basin, indicating that only 6 to 10 m of bioswale can mitigate a large proportion of metals in runoff. In addition, the EBK-generated heat maps display the location-specific infiltration and sequestration for each metal, in particular the two groups experiencing either monotonic decrease along the axis of water flow or reach a minimum in the center of the bioswale with higher concentrations at the north and south ends. Metals that increase in concentration at the south of the bioswale are found in short distance aerosols, such as brake pad wear, which enters the bioswale via a different source than the runoff from the north, whereas metals that monotonically decrease in concentration are not found in aerosol sources.

The clustering of metals generated through the PCA identified the metals the bioswale remediates most effectively, (cobalt, copper, lead, manganese, and zinc) as reinforced by linear regression models. Since these metals largely result from anthropogenic sources, strategically placed bioswales can be effective means to remove anthropogenic metals from stormwater runoff. The use of Principal Component Analysis allowed for an easy identification of metals most effectively remediated by the bioswale, and atomic emission spectroscopy allows for a large set of metals to be sampled rather than a handful. These findings extend research done by Leroy et al. (2016), Li et al. (2016), and others (Anderson et al., 2016, Delgard et al., 2012, Georgiev et al., 2016, Blecken et al., 2009, Davis, 2007, Hatt et al., 2009, Hunt et al., 2008), who studied fewer metals, by establishing PCA as a means for identifying pertinent metals within larger sets of measured pollutants.

This larger set of metals revealed that metals that are sequestered with statistical significance by the bioswale have elevated concentrations in the carbonate soil fraction. The degree that this increased affinity for the carbonate soil fraction contributes to their better sequestration is unclear, and the introduction of metals via aqueous runoff versus brake aerosol likely influences this data as well. Nonetheless, the study demonstrates that anthropogenic metals such as zinc, lead, cobalt, copper, and manganese can be effectively mitigated along the flow path of a bioswale. Furthermore, constructing bioswales with higher carbonate soil fractions, likely by supplementing the soil with calcite, may increase the ability of that bioswale to bioremediate metals in runoff.

Acknowledgments

Profs. Branwen Williams and Colin Robins (W. M. Keck Science Department of Claremont McKenna, Pitzer, and Scripps Colleges) and NSF MRI 1429620 for providing an ICP-OES, Prof. Warren Roberts (Claremont Graduate University), Prof. J. Travis Columbus (Rancho Santa Ana Botanical Garden), and Prof. Karl Haushalter (Harvey Mudd College) for assistance and instrumentation; Skyler Lewis, Boyu Liu, Paul Picciano, and Liana Solis from Pomona Class of 2016 for background research on this bioswale; and Seaman family for funding.

Conflicts of interest

The authors declare no conflicts of interest.

Appendix A. Supplementary data

Supplementary data to this article can be found online at https://doi.org/10.1016/j.scitotenv.2018.08.441.

References

Almeida, M., Mucha, A., Vaconcelos, T., 2004. Influence of the sea rush *Juncus maritimus* on metal concentration and speciation in estuarine sediment colonized by the plant. Environ. Sci. Technol. 38, 3112–3118.

Anderson, B., Phillips, B., Voorhhes, J., Siegler, K., Tjeerdema, R., 2016. Bioswales reduce contaminants associated with toxicity in urban storm water. Environ. Toxicol. Chem. 35 (12), 3124–3134.

Annu, Garg, A., Urmila, 2016. Level of Cd in different types of soil of Rohtak district and its bioremediation. J. Environ. Chem. Eng. 4, 3797–3802. https://doi.org/10.1016/j.jece.2016.08.023.

Blecken, G.-T., Zinger, Y., Deletić, A., Fletcher, D., Viklander, M., 2009. Impact of a submerged zone and a carbon source on heavy metal removal in stormwater biofilters. Ecol. Eng. 35 (5), 769–778.

Brown, Gordon E., Foster, Andrea L., Ostergren, John D., 1999. Mineral surfaces and bioavailability of heavy metals: a molecular-scale perspective. Proc. Natl. Acad. Sci. 96 (7), 3388–3395.

Chapman, C., Horner, R., 2010. Performance assessment of a street-drainage bioretention system. Water Environ. Res. 82 (2), 109–119.

Davis, A., 2007. Field performance of bioretention: water quality. Environ. Eng. Sci. 24 (8), 1048–1064.

Delgard, M.L., Beflandre, B., Metzger, E., Nuzzio, D., Capo, S., Mouret, A., Anschutz, P., 2012. In situ study of short-term variations of redox species chemistry in intertidal permeable sediments of the Arcachon lagoon. Hydrobiologia 699, 69–84. https://doi.org/Hydrobiologia.

Gadde, R.Rao., Laitinen, Herbert A., 1974. Heavy metal adsorption by hydrous iron and manganese oxides. Anal. Chem. 46 (13), 2022–2026.

Georgiev, P., Groudev, S., Spasova, I., Nicolova, M., 2016. Transport of radionuclides and heavy metals during the cleanup of a polluted cinnamonic soil. J. Geochem. Explor. 174, 148–158.

Grant, S., Rekhi, N., Pise, N., Reeves, R., Matsumoto, M., Wistrom, A., Moussa, L., Bay, S., Kayhanian, M., 2003. A Review of the Contaminants and Toxicity Associated with Particles in Stormwater Runoff. California Department of Transportation.

Hatt, B.E., Fletcher, T.D., Deletic, A., 2009. Pollutant removal performance of field-scale stormwater biofiltration systems. Water Sci. Technol. 59 (8), 1567–1576.

Hunt, W.F., Smith, J.T., Jadlocki, S.J., Hathaway, J.M., Eubanks, P.R., 2008. Pollutant removal and peak flow mitigation by a bioretention cell in urban Charlotte. N.C. J. Environ. Eng. 134 (5).

Kogut, Megan B., Voelker, Bettina M., 2003. Kinetically inert Cu in coastal waters. Environ. Sci. Technol. 37 (3), 509–518. https://doi.org/10.1021/es020723d.

Leroy, M.C., Marcotte, S., Legras, M., Moncond'huy, V., Le Derf, F., Portet-Koltalo, F., 2016. Influence of the vegetative cover on the fate of trace metals in the retention systems simulating roadside infiltration swales. Sci. Total Environ. 580, 482–490.

Lewis, S., Liu, B., Picciano, P., Solis, L., 2016. Bioswales for Stormwater Remediation and Infiltration: Assessing Regulatory Climate and Quantifying Filtration Capacity of a Claremont Bioswale. Environmental Analysis Program Senior Projects (May). http://scholarship.claremont.edu/eap_senior_projects/1.

Li, J., Jiang, C., Lei, T., Li, Y., 2016. Experimental study and simulation of water quality purification of urban surface runoff using non-vegetated bioswales. Ecol. Eng. 95, 706–713.

R Development Core Team, 2008. R: A Language and Environment for Statistical Computing. R Foundation for Statistical Computing, Vienna, Austria 3-900051-07-0 http://www.R-project.org.

Tessier, A., Campbell, P., Bisson, M., 1979. Sequential extraction procedure for the speciation of particulate trace metals. Anal. Chem. 51 (7), 844–851.

Zimmerman, A., Weindorf, D., 2010. Heavy metal and trace metal analysis in soil by sequential extraction: a review of procedures. Int. J. Anal. Chem. 2010, 1–7 (387803).